Rb atoms in a blue-detuned dipole trap: Coherence and ground-state differential ac Stark shift

D. Sheng,* J. Zhang, and L. A. Orozco
Joint Quantum Institute, Department of Physics, University of Maryland, and National Institute of Standards and Technology, College Park, Maryland 20742, USA
(Received 2 July 2012; revised manuscript received 22 May 2013; published 14 June 2013)

Blue-detuned dipole traps and their ability to preserve atomic coherences are interesting for precision measurement applications. In this paper, we present experimental studies on the differential ac Stark shift of the ground-state hyperfine splitting in ^{87}Rb atoms confined in a dynamic blue-detuned dipole trap. We systematically study the power and detuning effects on the Rabi resonance frequency (differential ac Stark shift) and its linewidth (coherence) and find that their performance is compatible with future parity violation experiments in Fr.

DOI: 10.1103/PhysRevA.87.063412 PACS number(s): 37.10.Gh, 37.10.Vz

I. INTRODUCTION

Optical dipole traps are a convenient way to confine cold neutral atoms for long-term spectroscopic interrogation. They operate in two general classes, the blue-detuned that traps atoms in the region with minimum intensity [1], and the red-detuned that traps atoms in the region of maximum intensity [2]. The blue-detuned trap minimizes perturbations to the objects under study, and makes it attractive in applications for precision measurements requiring good ground-state coherence or low scattering rates [3–9]. Their use in atomic clocks, with optical lattices, has triggered a large interest in their properties and how they affect the clock performance (see, for example, Ref. [10] and references therein). Blue traps also have a wide application in quantum information processing and coherent light storage (see, for example, Refs. [11,12]).

Our interest in a detailed study of atomic coherence in blue-detuned dipole traps resides in their potential use in our experimental efforts to work with Fr on weak interaction physics. The knowledge of its atomic properties is behind that of the other alkali atoms, but current experiments aimed at measuring the anapole moment require further atomic spectroscopy studies [6,13]. The anapole moment [14–16], a nuclear chiral current created by weak interactions between nucleons, is the dominant contribution to the nuclear spin-dependent weak interaction that causes parity nonconservation (PNC) in heavy atoms [15,17,18]; it can be thought of as a weak radiative correction among nucleons probed by an electromagnetic interaction [19]. The anapole moment makes $E1$ transitions possible among hyperfine ground-state levels. We are using radioactive Fr (nuclear charge $Z = 87$) [20], the heaviest alkali atom, as the anapole moment grows faster than Z. The Fr experiment is taking place at the Isotope Separator and Accelerator (ISAC) radioactive beam facility at TRIUMF in Vancouver, Canada.

The authors of Refs. [6,21] presented a detailed study of the experimental requirements, including possible sources of systematic effects that can mimic the PNC signal. Briefly, we are using interference between a parity conserving transition and a parity nonconserving one. We want to continuously drive an electromagnetically forbidden electric dipole ($E1$) transition between the two ground hyperfine states with a microwave field in a Fabry-Perot cavity while driving the allowed magnetic dipole ($M1$) transition with a field propagating in the direction perpendicular to the Fabry-Perot cavity axis. The microwave field that drives the $M1$ transition induces Rabi oscillations between the two ground-state hyperfine levels. The Rabi frequency is slightly modified by the weak interaction such that there is an increase (decrease) of the frequency depending on the handedness of the apparatus, allowing for the extraction of weak interaction physics. This continuous driving scheme is in contrast to the Ramsey method where the excitation is pulsed. A Ramsey measurement uses the phase accumulated between pulses to give the energy separation between two atomic levels but not the transition strength.

This paper presents tests of the performance of the blue-detuned dipole trap we are planning to use in the PNC measurements and complements our recent paper on the interference method sensitivity test [22]. We need to understand the effects of the blue-detuned dipole trap on the atom hyperfine energy levels and its influence on the coherence properties of a superposition of the two hyperfine states. There is also a close relation between the atomic dynamics and the atom superposition coherence properties inside a blue-detuned dipole trap [23], through their dependence on the shape of the trap boundaries. This fact also plays an important role in the study of neutron traps [24,25] for permanent electric dipole moment (EDM) searches. We present in a separate publication the study on the dynamics of the trapped atoms when probed as classical hard objects and when probed using their internal quantum degrees of freedom [26].

Long coherence of the superposition (narrow Rabi resonance) has been identified as critical for future precision measurements such as the observation of time-reversal violation in atoms [27,28]. The atoms should be trapped with the minimum disturbance to their coherence properties. Our dipole trap aims to decrease the photon scattering, damaging to the coherence, and differential ac Stark shift introduced by the trapping laser. We use a far off-resonance trap (FORT) to reduce the photon scattering rate and choose a blue-detuned trap where the atoms are confined on the minima of the light field, the so-called dark region of the trap. The ac Stark shift depends on various parameters, including the position of atoms in the trap, the atomic state, and the interaction time. We

*Present address: Department of Physics, Princeton University, Princeton, NJ 08544, USA.

present here a detailed spectroscopic study of the effects of the blue-detuned trap on a coherent superposition of ^{87}Rb atoms in their hyperfine ground state, and our results can then be scaled to the other alkali, in particular to Fr.

As we gain theoretical [29] and experimental knowledge of the scalar, vector, and tensor polarizabilities in Fr, it may be possible to find magic wavelengths [10] to further suppress the differential ac Stark shift. The authors of Refs. [30,31] showed such a realization in the ground-state hyperfine levels of ^{87}Rb.

The paper has four sections after this Introduction. Sections II and III have brief reviews of the theory and the apparatus involved in the measurement. Section IV presents the measurements, and Sec. V has a summary and conclusion.

II. THEORETICAL CONSIDERATIONS FOR ATOMIC TRAP

The potential U felt by an atom in a dipole trap depends on the full atomic polarizability α and the position-dependent intensity $I(\mathbf{r})$ [2]

$$U(\mathbf{r}) = -\frac{1}{2\epsilon_0 c}\mathrm{Re}(\alpha) I(\mathbf{r}). \tag{1}$$

The specific structure of α, with its scalar, vector, and tensor parts, can give rise to enhancements and cancellations that shape both the ground and excited states addressed by the trapping light [10].

When a measurement involves both hyperfine states of the atoms, as is our case here, the presence of the dipole trap makes a small difference in the ac Stark shift of these two ground states due to the different atomic detunings of the two states and their different atomic polarizabilities α. This is the so-called differential ac Stark shift ($\delta_{\mu W}$), and it changes the hyperfine energy splitting ($\hbar\omega_{\mathrm{HF}}$) by $\Delta U_{\mathrm{HF}}(\mathbf{r})$. When the generalized trap laser detuning from the excited state δ is large compared to ω_{HF}, using $U(\mathbf{r})$ from Eq. (1) the differential ac Stark shift is

$$\Delta U_{\mathrm{HF}}(\mathbf{r}) = -\frac{\omega_{\mathrm{HF}}}{\delta} U(\mathbf{r}). \tag{2}$$

Although the ac Stark shift has opposite signs for the red- and blue-detuned dipole traps, the differential shift $\Delta U_{\mathrm{HF}}(\mathbf{r})$ is negative for both cases, always decreasing the hyperfine splitting.

There are several different optical configurations for generating blue-detuned traps [1,7]. In this work, we use a rotating dipole trap because we can control the shape and size dynamically. The general expression of the time-averaged potential $U(\rho,z)$ for linearly polarized light and a detuning much larger than the hyperfine splittings is [32]

$$U(\rho,z) = \frac{\hbar\gamma}{24 I_S}\left[\frac{1}{\delta_{1/2}/\gamma} + \frac{2}{\delta_{3/2}/\gamma}\right]\frac{\oint_{\rho'\in\mathcal{L}} I(\rho-\rho',z)dl}{\oint dl}, \tag{3}$$

where γ is the natural linewidth of the ^{87}Rb D_2 transition, I_S is the saturation intensity $I_S = 2\pi^2\hbar c\gamma/(3\lambda^3)$ with λ the transition wavelength, and $I(\rho,z)$ is the Gaussian beam intensity at position (ρ,z). The integral over the rotating laser beam contour $\mathcal{L}$ gives the time-averaged potential, and in most cases, this integral does not have an analytic expression and needs numerical calculation. The expression for the detuning δ now involves $\delta_{1/2}$ ($\delta_{3/2}$) refering to the detuning from the D_1 (D_2) line. The equation above assumes that the contour is scanned uniformly in time, which needs special attention when generating irregular trap shapes.

III. APPARATUS AND METHODS

A laser rotating faster than the motion of the atoms creates a time-averaged potential equivalent to a hollow beam potential [33,34]. The laser beam propagating in the z direction goes through two acoustooptical modulators (AOMs) placed back-to-back with the crystal direction perpendicular to each other. We use the beam that corresponds to the first diffraction order in both directions, the (1,1) mode. We scan the modulation frequency of both AOMs with two phase-locked function generators (Stanford Research SRS DS345) to generate different hollow beam shapes. Tightly focusing the laser at the position of the atoms confines them along the beam axis. The authors of Ref. [21] have a detailed study of trap lifetime, potential, and power lock.

The ^{87}Rb atoms are first captured in a magnetooptical trap (MOT) from a thermal gas produced by a dispenser. The background pressure in the chamber allows MOT lifetimes of tens of seconds. After capture, the polarization gradient (optical molasses) cools the atoms to a temperature of 15 μK. The trap resides inside a large stainless steel vacuum chamber with multiple windows. Details of the trap are available in Ref. [35]. We load atoms into the blue-detuned trap by turning the trap on in the presence of cooling beams (optical molasses).

We interrogate the atoms through the magnetic dipole $M1$ transition freely expanding or trapped in the presence of a bias field of 0.5 G to define the quantization axis. The states involved in the $M1$ transition are the two ground clock states ($|F=1,m_F=0\rangle$ and $|F=2,m_F=0\rangle$) of ^{87}Rb. We generate this frequency by mixing a 6820-MHz microwave-frequency signal from a HP 8672A signal generator and a radio-frequency signal from a SRS DS345 function generator, where both generators are phase locked with each other. We drive the microwave transition for a given time, then we optically excite the atoms from a given hyperfine state and use a Hamamatsu R636 photomultiplier tube (PMT) to detect the florescence, which is proportional to the atom number in each state. The number of the atoms left depends on the trap potential. We have 10^5 atoms left after a 40-ms interaction time for the largest detuning in our experiment. The evolution of the atoms between the two hyperfine levels follows damped Rabi oscillations [22]. We measure the probability of atoms in the state $|2\rangle$ using the state selective detection method [23], where we first measure the number of atoms in $|5S,F=2\rangle$ by driving a cycling transition to $|5P_{3/2},F=3\rangle$, then we turn on another laser beam on resonance with $|5S,F=1\rangle \rightarrow |5P_{3/2},F=1\rangle$ together with the previous cycling transition and measure the total number of atoms.

We adopt the echo spectroscopy to study the relation between the orbits and coherence [23]. This method consists of a microwave echo sequence ($\pi/2$-π-$\pi/2$) with a time delay τ between each pulse. Due to the motion of the atoms and the position dependence of $\Delta U_{\mathrm{HF}}(\mathbf{r})$, the dephasing caused by the differential ac Stark shift is time dependent and related to

the atomic orbit. Suppose that one atom starts in one of the clock states, during the echo sequence, the relative phase between two clock states accumulated in first τ time (ϕ_1) and sencond τ time (ϕ_2) is different by an amount of $\Delta\phi$. We measure the probability of the atom ending in the other clock state after the echo sequence, which is $\sin^2(\Delta\phi/2)$ [26]. In the measurement result, we could observe a revival in this quantum correlation decay signal as we scan τ, whose amplitude measures the overlap between two nearby orbits in time. This method is especially useful to compare the properties of coherence due to a change on the trap shape.

IV. MEASUREMENTS

We map the differential ac Stark shift of atoms by finding the resonance in the Rabi oscillations ($\delta_{\mu w}$) between clock states for different potentials. We first measure the unperturbed hyperfine splitting using the cold atoms released from the MOT in the absence of the dipole trap. The effect of gravity limits us to a 15-ms interaction time. When the dipole trap is on, we have a longer interaction time t_R. We choose 40 ms which limits the transit-time broadening line width to 22 Hz ($0.89/t_R$). We turn on the dipole trap 20 ms before turning off the MOT beam, with the trap beam waist of 30 μm. We use a transverse square shape (210 μm per side) dipole trap in the measurement with the diagonal line in the direction of gravity shown in the inset of Fig. 1). The total power in the dipole trap for these measurements is 530 mW with a maximum intensity of 2.1×10^6 mW/cm^2 [I in Eq. (3)].

We study the differential shift of the hyperfine levels for several trap detunings while keeping the trapping beam power constant for all the detunings and plot three examples of experimental results in Fig. 1. The measurements show that for the free expanding atoms the line shape is symmetric and the linewidth is limited by the interaction time (black squares). The line shape is asymmetric in the presence of the trap, especially when the detuning is small (blue filled circles).

We first focus on the position of the differential shift peak and plot its relation to the detuning in Fig. 2. We need to be careful about the application of Eq. (2) to interpret the data,

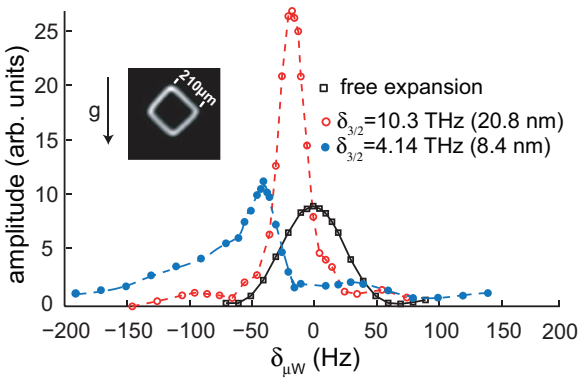

FIG. 1. (Color online) Rabi oscillation amplitude as a function of detuning that shows the differential ac Stark shift. The free expansion is the symmetric shape with black filled squares. The red circles and blue filled circles are for a blue detuned trap. The transverse shape of the trap is in the inset picture with the arrow indicating the direction of gravity.

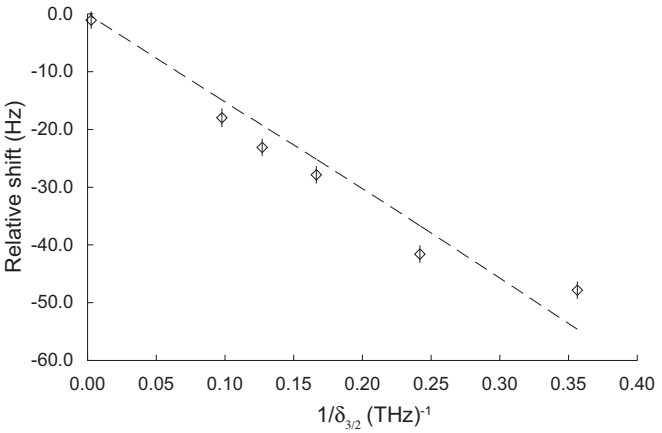

FIG. 2. Ground-state differential ac Stark shift as a function of the trap detuning $\delta_{3/2}$. The dashed line is a fit using Eq. (4) to guide the eye.

which seems to conclude that the position of the peak should be proportional to $1/\delta^2$ because $U(\mathbf{r})$ is inversely proportional to δ. However, the result in Fig. 2 is much closer to $1/\delta$. This is a difference from the red-detuned traps, where atoms reside in the maximum intensity region, and every atom feels the change in the potential independent of its kinetic energy. In the case of the blue-detuned trap, atoms are trapped in the minimum intensity region of the trap, so that the maximum potential atoms could feel is limited by their kinetic energy. The decrease in the trap potential leads to the escape of atoms with high kinetic energy, but only slightly affects atoms still left in the trap. In other words, Eq. (2) still holds, but $U(\mathbf{r})$ is the averaged potential over the atomic trajectory. A simpler expression that takes into account the contribution of the two $5p$ states to the polarizability α through the detuning to both D_1 and D_2 lines is

$$\Delta U_{\mathrm{HF}} = \omega_{\mathrm{HF}} \left(\frac{1}{\delta_{3/2}} \frac{2\delta_{1/2}}{\delta_{3/2} + 2\delta_{1/2}} + \frac{1}{\delta_{1/2}} \frac{\delta_{3/2}}{\delta_{3/2} + 2\delta_{1/2}} \right) E_k, \tag{4}$$

where E_k is the sum of the kinetic energy and gravitational energy of the atoms, and the subscripts on δ refer to the appropriate p state. Figure 2 shows (dashed line) the fit of the data to Eq. (4).

We further study the effects on the differential ac Stark shift ($\delta_{\mu W}$) from the potential well depth by increasing and decreasing the trap beam power by a factor of 2 while fixing the detuning $\delta_{3/2} = 2.81$ THz (5.7 nm). We see no change of the peak position within ± 1.5 Hz.

Another important parameter is the linewidth of the Rabi resonance from the differential ac Stark shift distribution, which determines the decoherence rate of the trap. Figure 3 shows the full width at half maximum (FWHM) and the half width at half maximum (HWHM) for the blue and red sides of the Rabi resonance as a function of detuning for the same experimental parameters as in Fig. 2.

A simple description of the linewidth (d) is the result of two contributions:

$$d = \sqrt{d_t^2 + b^2(\delta) d_k^2}, \tag{5}$$

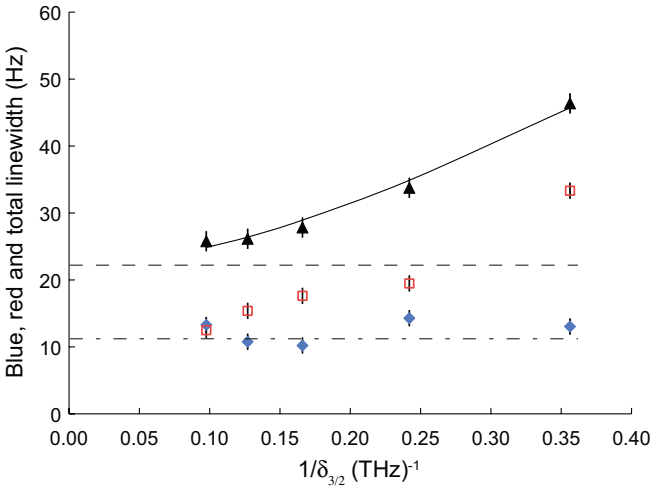

FIG. 3. (Color online) Linewidth of the Rabi resonances as a function of blue trap detuning ($\delta_{3/2}$). Blue rhombi show the HWHM on the blue side of resonance. Red squares show HWHM on the red side of resonance. Black triangles show the FWHM of the resonance with a fit to Eq. (5) to guide the eye. The dashed dotted (dashed) line is the transit time broadening limit d_t HWHM (FWHM).

where d_t is the transit time broadening limit, d_k is the linewidth due to the kinetic energy distribution, and $b(\delta)$ is the scaling factor which scales inversely with the generalized trap laser detuning δ. The effects of the kinetic energy distribution have been discussed for both red- and blue-detuned dipole traps [36,37]. The differential ac Stark shift is a time-averaged effect because atoms are moving around. The energy shift is proportional to the trap potential that the atoms feel, weighed by the time atoms spend in that region. Atoms with a smaller kinetic energy feel a smaller trap potential, but they also have to be trapped on the lower side of the trap where the dark region is smaller. Atoms with a higher kinetic energy see a higher trap potential, but they have a larger dark region to move around, which leads to the result that the time-averaged effect does not exactly reflect the velocity distribution. However, Eq. (5) qualitatively describes the behavior as the fit (continuous line) shows in Fig. 3. On the blue side of the differential shift distribution, over the detuning range in this paper, the linewidth is dominated by d_t (dashed dot line in Fig. 3). The red side has a much broader velocity distribution, and its linewidth at small trap detuning is mainly due to the movement of the atoms. As the detuning increases, its linewidth also converges to d_t.

We also study the relation between atomic movement and the differential ac Stark shift through a simulation for two different shapes of traps. The simulation follows the Rabi oscillations of many atoms as they dynamically probe a trap potential of 25 μK and $\delta_{3/2} = 2.81$ THz (5.7 nm) blue-detuned from the D_2 line to understand the asymmetry (see Fig. 4). We use Eq. (2) for the differential ac Stark shift. The result reproduces the shift of the resonance peak (black continuous trace). We convolve the result with a 40-ms pulse in frequency space (set by the interrogation time of the atoms). The asymmetry coming from the atom movement (red dashed trace) remains.

The simulation of the Rabi resonances in a dipole trap (shape 1) also shows two peaks [see Fig. 4(a)], one is around -50 Hz and the other one is around -100 Hz; however, experimentally we only observe the first peak, whose broad line shape on the red side has a contribution from the unresolved second peak. Figure 4(b) shows the results for different interaction time, with no double peak at the beginning, and a doublet after 20 ms. A detailed series of simulations shows that there are four kinds of orbits [Fig. 4(c)] that contribute to the observed first peak. By adding a small linear barrier (barrier length is 30 μm) in the middle of the trap [shape 2 in Fig. 4(a)], we destroy the latter three kinds of stable orbits, so that only one peak around -100 Hz remains [the blue dotted curve in Fig. 4(a)].

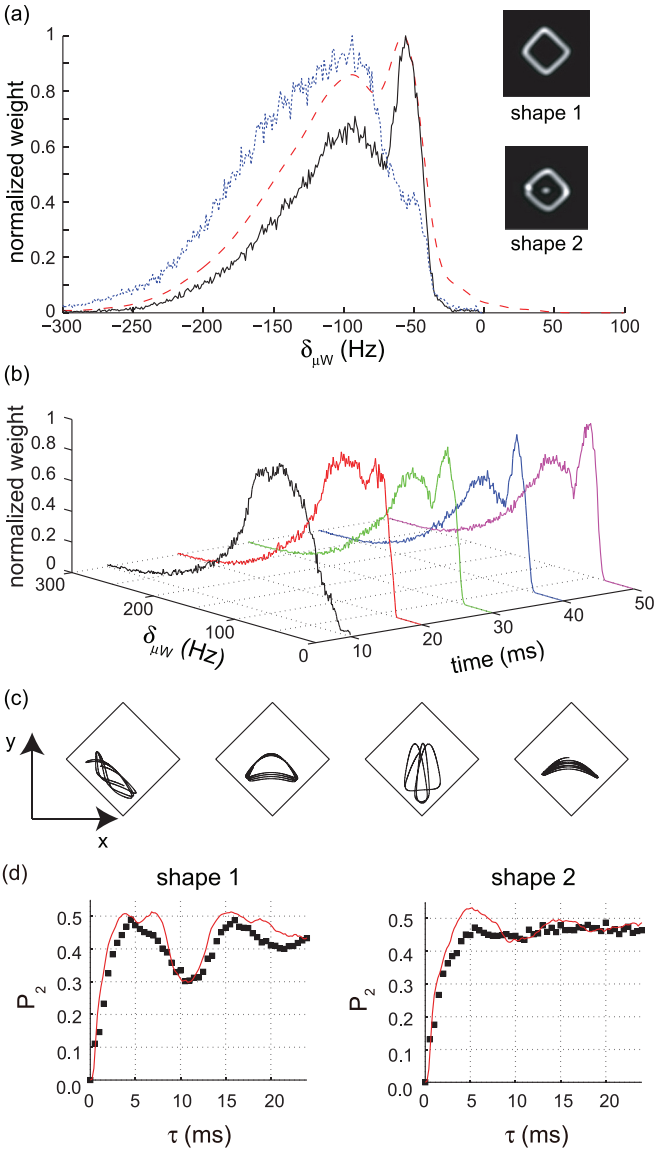

FIG. 4. (Color online) (a) Rabi resonance simulation of atoms with an interaction time of 40 ms in a dipole trap with two shapes (shape 1, black continuous line; shape 2, blue dotted line) and the convolution of the shape 1 results with the 40-ms pulse (dashed red line). (b) Simulation results of the differential ac Stark shift with different interaction times for shape 1 dipole trap. (c) Four kinds of atomic orbits that contribute to the peak at -53 Hz of shape 1 dipole trap in panel (a). (d) Experimental (black) and theoretical (red) results of echo spectroscopy on atoms inside the dipole trap with both shapes.

The big difference in the linewidth of the two peaks also suggests that the coherence property changes dramatically by adding this barrier. We experimentally implement the echo spectroscopy mentioned in the previous section, and show the results in Fig. 4(d). The obvious decrease in the revival amplitude confirms that the presence of the barrier destroys largely the overlap of the nearby orbits and in turn the coherence of the trap.

We will address a more detailed and systematic study on the close connection among the atomic dynamics, the trap shape, and the coherence properties of the atoms in the blue-detuned dipole trap in a different publication [26].

V. SUMMARY AND CONCLUSION

The differential ac Stark shift and coherence properties of the blue-detuned dipole trap as measured by Rabi oscillations of ground-state superpositions in ^{87}Rb are encouraging for use of blue-detuned dipole traps in anapole PNC experiments [21,22]. The use of magic wavelengths in Fr is an interesting possibility [10] that needs further study. Francium polarizabilities are not yet measured and some of the low-lying states such as the $6d$ have not been found.

When working with Rb and the detuning is 10 THz (20 nm) blue from the D_2 line we reach 180 ms of coherence lifetime t_c with a Rabi frequency of the driving field of $2\pi \times 46.8$ rad/s and observe a differential ac Stark shift of 18 Hz [22]. Francium atoms have, however, almost seven times larger hyperfine splitting (neutron-deficient isotopes with lifetime greater than 1 min) [13], so we need a larger detuning for the trapping laser in the Fr experiment to get similar results as with Rb. We want to emphasize that, due to the interference experimental scheme [22], the microwave field that drives parity allowed $M1$ transition is always on, in contrast with the pulses encountered using the Ramsey method [3]. Decoherence can come from the imperfections of the driving microwave field, such as field gradients. However, our Fr apparatus works in the quasi-optical regime with a geometry that allows great control over phase and amplitude.

The achievable experimental conditions with a 532-nm laser corresponding to a detuning $\delta > 70$ THz (120 nm), with a cold sample of Fr atoms, are promising for the PNC experiment. There are still possible complications in Fr as its energy levels and ionization potential are different from Rb.

The ultimate question of signal-to-noise ratio (S/N) is important. Under very general considerations, independent of the measurement methods as long as the correlation between atoms in this system decays exponentially [38,39], the S/N scales as $\sqrt{N_a \times t \times t_c}$, where N_a is atom number, t is the total measurement time, and t_c is the coherence time of the system. An increase of the coherence time without changing the atom number has the same effect of the increase of integration time, which is the essence of our proposal compared to the previous experiments using hot atoms [40]. In the real experiment, the period of each Fr collection cycle ($\sim$10 s) [20] is long compared to the coherence time, so the increase of coherence time is also important to increase the duty cycle.

ACKNOWLEDGMENTS

We thank E. Gomez, A. Pérez Galván, W. D. Phillips, and J. V. Porto for helpful discussions, and J. A. Groover for a careful reading of the manuscript. This work is supported by NSF and DOE.

[1] N. Friedman, A. Kaplan, and N. Davidson, Adv. At. Mol. Opt. Phys. **48**, 99 (2002).
[2] R. Grimm, M. Weidemüller, and Y. B. Ovchinnikov, Adv. At. Mol. Opt. Phys. **42**, 95 (1999).
[3] N. Davidson, H. J. Lee, C. S. Adams, M. Kasevich, and S. Chu, Phys. Rev. Lett. **74**, 1311 (1995).
[4] S. Kulin, S. Aubin, S. Christe, B. Peker, S. L. Rolston, and L. A. Orozco, J. Opt. B: Quantum Semiclass. Opt. **3**, 353 (2001).
[5] L. Khaykovich, N. Friedman, S. Baluschev, D. Fathi, and N. Davidson, Europhys. Lett. **50**, 454 (2000).
[6] E. Gomez, S. Aubin, G. D. Sprouse, L. A. Orozco, and D. P. DeMille, Phys. Rev. A **75**, 033418 (2007).
[7] S. E. Olson, M. L. Terraciano, M. Bashkansky, and F. K. Fatemi, Phys. Rev. A **76**, 061404 (2007).
[8] M. L. Terraciano, M. Bashkansky, and F. K. Fatemi, Phys. Rev. A **77**, 063417 (2008).
[9] G. Li, S. Zhang, L. Isenhower, K. Maller, and M. Saffman, Opt. Lett. **37**, 851 (2012).
[10] A. Derevianko and H. Katori, Rev. Mod. Phys. **83**, 331 (2011).
[11] M. Saffman, T. G. Walker, and K. Mølmer, Rev. Mod. Phys. **82**, 2313 (2010).
[12] K. Hammerer, A. S. Sørensen, and E. S. Polzik, Rev. Mod. Phys. **82**, 1041 (2010).
[13] E. Gomez, L. A. Orozco, and G. D. Sprouse, Rep. Prog. Phys. **69**, 79 (2006).
[14] Y. B. Zel'dovich, Sov. Phys. JETP **6**, 1184 (1958).
[15] V. V. Flambaum, I. B. Khriplovich, and O. P. Sushkov, Phys. Lett. B **146**, 367 (1984).
[16] J. S. M. Ginges and V. V. Flambaum, Phys. Rep. **397**, 63 (2004).
[17] O. P. Sushkov, V. V. Flambaum, and I. B. Khriplovich, Sov. Phys. JETP **60**, 873 (1984).
[18] M. A. Bouchiat and C. Bouchiat, Rep. Prog. Phys. **60**, 1351 (1997).
[19] V. V. Flambaum and D. W. Murray, Phys. Rev. C **56**, 1641 (1997).
[20] S. Aubin, E. Gomez, L. A. Orozco, and G. D. Sprouse, Rev. Sci. Instrum. **74**, 4342 (2003).
[21] D. Sheng, L. A. Orozco, and E. Gomez, J. Phys. B **43**, 074004 (2010).
[22] D. Sheng, J. Zhang, and L. A. Orozco, Rev. Sci. Instr. **83**, 043106 (2012).
[23] M. F. Andersen, A. Kaplan, T. Grünzweig, and N. Davidson, Phys. Rev. Lett. **97**, 104102 (2006).
[24] J. M. Pendlebury, W. Heil, Y. Sobolev, P. G. Harris, J. D. Richardson, R. J. Baskin, D. D. Doyle, P. Geltenbort, K. Green, M. G. D. van der Grinten, P. S. Iaydjiev, S. N. Ivanov, D. J. R. May, and K. F. Smith, Phys. Rev. A **70**, 032102 (2004).

[25] S. Paul, Nuc. Instr. Meth. A **611**, 157 (2009).
[26] D. Sheng, A. P. Galván, J. Zhang, and L. A. Orozco, (unpublished).
[27] C. Chin, V. Leiber, V. Vuletic, A. J. Kerman, and S. Chu, Phys. Rev. A **63**, 033401 (2001).
[28] M. V. Romalis and E. N. Fortson, Phys. Rev. A **59**, 4547 (1999).
[29] U. I. Safronova, W. R. Johnson, and M. S. Safronova, Phys. Rev. A **76**, 042504 (2007).
[30] N. Lundblad, M. Schlosser, and J. V. Porto, Phys. Rev. A **81**, 031611 (2010).
[31] R. Chicireanu, K. D. Nelson, S. Olmschenk, N. Lundblad, A. Derevianko, and J. V. Porto, Phys. Rev. Lett. **106**, 063002 (2011).
[32] S. J. M. Kuppens, K. L. Corwin, K. W. Miller, T. E. Chupp, and C. E. Wieman, Phys. Rev. A **62**, 013406 (2000).
[33] N. Friedman, L. Khaykovich, R. Ozeri, and N. Davidson, Phys. Rev. A **61**, 031403 (2000).
[34] P. Rudy, R. Ejnisman, A. Rahman, S. Lee, and N. Bigelow, Opt. Express **8**, 159 (2001).
[35] D. Sheng, A. Pérez Galván, and L. A. Orozco, Phys. Rev. A **78**, 062506 (2008).
[36] S. Kuhr, W. Alt, D. Schrader, I. Dotsenko, Y. Miroshnychenko, A. Rauschenbeutel, and D. Meschede, Phys. Rev. A **72**, 023406 (2005).
[37] M. L. Terraciano, S. E. Olson, and F. K. Fatemi, Phys. Rev. A **84**, 025402 (2011).
[38] S. F. Huelga, C. Macchiavello, T. Pellizzari, A. K. Ekert, M. B. Plenio, and J. I. Cirac, Phys. Rev. Lett. **79**, 3865 (1997).
[39] B. M. Escher, R. L. de Matos Filho, and L. Davidovich, Nat. Phys. **7**, 406 (2011).
[40] C. S. Wood, S. C. Bennett, D. Cho, B. P. Masterson, J. L. Roberts, C. E. Tanner, and C. E. Wieman, Science **275**, 1759 (1997).